Nonlin. Processes Geophys. Discuss., doi:10.5194/npg-2016-21, 2016
Manuscript under review for journal Nonlin. Processes Geophys.
Published: 11 April 2016

Nonlinear Processes in Geophysics
Open Access
Discussions

Constraining ecosystem model with Adaptive Metropolis algorithm using boreal forest site eddy covariance measurements

Jarmo Mäkelä[1], Jouni Susiluoto[1], Tiina Markkanen[1], Mika Aurela[1], Ivan Mammarella[2], Stefan Hagemann[3], and Tuula Aalto[1]

[1]Finnish Meteorological Institute, P.O. Box 503, 00101 Helsinki, Finland
[2]Department of Physics, P.O. Box 48, 00014 University of Helsinki, Finland
[3]Max Planck Institute for Meteorology, Bundesstraße 53, 20146 Hamburg, Germany

Correspondence to: Jarmo Mäkelä (jarmo.makela@fmi.fi)

Abstract. We examined parameter optimization in JSBACH ecosystem model, applied for two boreal forest sites in Finland. We identified and tested key parameters in soil hydrology and forest water and carbon exchange related formulations and optimized them using the Adaptive Metropolis algorithm for a five year calibration period (2000–2004) followed by a four year validation period (2005–2008). We were able to improve the modelled seasonal, daily and diurnal cycles of gross primary production and evapotranspiration but unable to enhance the models response to dryness. The improvements are mostly accounted for by parameters related to the ratio of leaf internal CO_2 concentration to external CO_2, relative humidity, transpiration and soil moisture stress.

1 Introduction

Inverse modelling of ecosystem model parameters against in situ observations is an established way to tune model parameters (see e.g. Scharnagl et al., 2011). As observation sites have their own characteristics, it is necessary to make local site simulations for model evaluation and calibration as they may reveal new insight into model behaviour and promote further development. Model-data fusion has been applied for boreal forest sites by e.g. Peltoniemi et al. (2015a), Wu et al. (2011), Thum et al. (2007 and 2008) and Aalto et al. (2004).

In this study we perform site level parameter optimization in the JSBACH model (Reick et al., 2013, see also Knorr et al., 2005 and Kaminski et al., 2013). JSBACH is the land surface component of the Earth System model of Max Planck Institute for Meteorology (MPI-ESM), used to simulate water and carbon storages and fluxes in the soil-vegetation-atmosphere continuum. The water and carbon fluxes are coupled in the model and thus modification of parameters related to one component usually has an effect on the others as well. The optimization process and the optimized values are also affected by the assimilation frequency and interval in minimizing the model-data mismatch. This effect can be studied in numerous ways e.g. Santaren et al. (2014) varied the length of assimilation interval while Matheny et al. (2014) focused on the diurnal error patterns.

The motivation for this study comes from results showing that CMIP5 model simulations, one of which is MPI-ESM, have systematic evapotranspiration biases over continental areas (Mueller and Seneviratne 2014). These kinds of biases have significant implications for climate change projections (Boé and Terray, 2008) but also have distinctive behaviour on a regional scale.

In addition a comparative study of the Gross Primary Production (GPP) of Finnish forests (Peltoniemi et al., 2015b) revealed that JSBACH has an insufficient response to water limitation in Finland – it tends to overestimate GPP and evapotranspiration during dry periods. This is especially apparent in the dry year 2006 as JSBACH is unable to transfer the reduced rainfall into lower levels of GPP.

In this study we apply the JSBACH ecosystem model for Hyytiälä (Kolari et al., 2009 and Suni et al., 2003) and Sodankylä (Thum et al., 2008 and Aurela, 2005) sites. We identify key parameters in soil hydrology and evapotranspiration related formulations and test their effectiveness with elementary methods. We study the effect of different timescales (seasonal, daily and half-hourly) on the assimilation process and the effect of this on the optimized parameter values. Several optimizations are performed using the Adaptive Metropolis (AM) algorithm during a five year calibration period (2000–2004) followed by a four year validation period (2005–2008).

The goals of this study are to test the applicability of the AM optimization method for JSBACH and the impact of different temporal resolutions on the optimization process, and to improve the models response to environmental drivers, focusing on dryness.

2 Materials and methods

2.1 Measurement sites and instrumentation

In this study we use site level data from two Finnish measurement sites: Hyytiälä (61°51'N, 24°17'E, 180 m a.s.l.) and Sodankylä (67°22'N, 26°38'E, 179 m a.s.l.). These well-established sites have long continuous measurement data sets representing well the southern and northern boreal Finnish coniferous evergreen forests. The data used in this study is available for the scientific community through various databases such as FLUXNET (doi:10.17616/R36K9X).

Hyytiälä site is a Finnish Scots pine (*Pinus sylvestris*) forest (Kolari et al., 2009), planted in 1962 after burning and mechanical soil preparation. The soil type in Hyytiälä is *Haplic Podzol* on glacial till and the site is of medium fertility (Kolari et al., 2009). The forest also has sparse understory of Norway Spruce (*Picea abies*) and scattered deciduous trees. The maximum of measured all-sided leaf area index (LAI) is 6.5 m^2 m^{-2} for the Scots pine. The carbon dioxide (CO_2) and water vapour (H_2O) fluxes between vegetation and atmosphere has been measured in Hyytiälä continuously since 1997 (Vesala et al., 2005).

The Sodankylä forest, at Sodankylä at the Finnish Meteorological Institute's Arctic Research Centre, is also a Scots pine forest (*Pinus sylvestris*) with maximum measured LAI of 3.6 m^2 m^{-2} as determined from a forest inventory in early autumn (Thum et al., 2007). The forest on *Fluvial Sandy Podzol* has been naturally regenerated after forest fires with tree age ranging approximately from 50 to 100 years. The sparse ground vegetation consists of lichens (73%), mosses (12%) and ericaceous shrubs (15%). The CO_2 and H_2O flux measurements in Sodankylä have been running since 2000 (Aurela 2005).

The CO_2 fluxes were measured by the micrometeorological eddy covariance (EC) method which provides direct measurement of CO_2 exchange between atmosphere and biospheres averaged on an ecosystem scale. In the EC method, the CO_2 flux is obtained as the covariance of the high frequency (10 Hz) observations of vertical wind speed and the CO_2 concentration (Baldocchi 2003). The EC instrumentation in Hyytiälä consisted of a Solent 1012R3 three-axis sonic anemometer (Gill Instruments

Nonlin. Processes Geophys. Discuss., doi:10.5194/npg-2016-21, 2016
Manuscript under review for journal Nonlin. Processes Geophys.
Published: 11 April 2016

Nonlinear Processes in Geophysics
Open Access
Discussions

Ltd., Lymington, UK) and a LI-6262 closed-path CO_2/H_2O gas analyser (Li-Cor Inc., Lincoln, NE, USA), while in Sodankylä a USA-1 (METEK GmbH, Elmshorn, Germany) anemometer and a LI-7000 (Li-Cor., Inc., Lincoln, NE, USA) closed path gas analyser was used. The EC fluxes were calculated as half-hourly averages taking into account the required corrections. The measurement systems and the post-processing procedures are presented in more detail for Hyytiälä (Kolari et al., 2004 and Mammarella et al., 2009) and Sodankylä (Aurela, 2005 and Aurela et al., 2009).

2.2 The JSBACH model

In JSBACH the land surface is a fractional structure where the land grid-cells are divided into tiles representing the most prevalent vegetation classes called plant functional types (PFTs) within each grid cell (Reick et al., 2013). The grid cell is first divided into bare soil and vegetative area which is furthermore fractionally divided into PFTs. The model was setup to effectively use only one tile, coniferous evergreen trees. Henceforth all model and process descriptions are considered in relation to coniferous evergreen trees and no distinction between PFT specific and general parameters are made in this study.

Coniferous evergreen trees are characterized by a set of parameters that control vegetation related biological and physical processes accounting for the land-atmosphere interactions. We made use of expert knowledge to set these parameters for our local sites and verified that they are in line with those presented by Hagemann (2002) and Hagemann and Stacke (2015).

The seasonal development of LAI is regulated by air temperature and soil moisture with a specific maximum LAI as a limiting value. The cycle is driven by a pseudo soil temperature that is a weighted running mean of air temperature. The predictions of phenology are produced by the Logistic Growth Phenology (LoGro-P) model of JSBACH.

Photosynthesis is described by the biochemical photosynthesis model (Farquhar et al., 1980). Following Kattge et al. (2009) we set the maximum carboxylation rate at 25 degrees Celsius to 1.9 times the maximum electron transport rate at 25 degrees Celsius.

The photosynthetic rate is resolved in two steps. First the stomatal conductance under conditions with no water stress is assumed to be controlled by photosynthetic activity (Schulze et al., 1994). Here the leaf internal CO_2 concentration is assumed to be a constant fraction of ambient concentration which allows for an explicit resolution of the photosynthesis (see e.g. Knorr 1997). Then the impact of soil water availability is accounted for by a soil moisture dependent multiplier that is identical for each canopy layer (Knorr 1997).

Radiation absorption is estimated by a two stream approximation within a three-layer canopy (Sellers 1985). Especially in the sparse canopies the radiation absorption is affected by clumping of the leaves which is here taken into account according to the formulation by Knorr (1997).

The JSBACH model was used uncoupled from the atmosphere and other components of the full MPI-ESM. We use half-hourly measurements from years 1999–2008 for Hyytiälä. The measurement interval is looped over to generate a 30 year spin up to accumulate sufficient soil moisture content and LAI. The spin up finishes at the end of 1999 and is followed by a calibration period of 2000–2004 and a validation period of 2005–2008, including an exceptionally dry summer in 2006. The setup for Sodankylä is similar but we use measurements from 2000–2008, where the spin up finishes at the end of 2008. The model is then restarted from the start of 2000 and we only examine the validation period (2005–2008) for Sodankylä.

Nonlin. Processes Geophys. Discuss., doi:10.5194/npg-2016-21, 2016
Manuscript under review for journal Nonlin. Processes Geophys.
Published: 11 April 2016

Nonlinear Processes in Geophysics
Discussions

The meteorological data used to drive the climate were air temperature, air pressure, atmospheric CO_2 concentration, precipitation, specific humidity, short- and longwave radiation, potential shortwave radiation and wind speed.

2.3 The parameters

The JSBACH model was modified to fit our custom-built testbed so that all parameters of interest could be read from an external file. We examined 15 parameters (Table 1) that are for convenience separated into three classes. Specific parameters for coniferous evergreen trees or the grid cell are in class I. These parameters are used only for seasonal tuning of the model and can be considered as site specific. Class II consists of general parameters and those in class III are specific for LoGro phenology model.

2.4 Parameter estimation

The parameter estimation in this study was done with the Adaptive Metropolis (AM) algorithm which produces the posterior probability distributions for the parameters using Bayesian methods. The AM algorithm is an adaptive Markov Chain Monte Carlo (MCMC) process described below (it is not strictly Markovian but satisfies the necessary ergodicity requirements). The rigorous mathematical presentation of the AM algorithm is presented in detail in Haario et al. (2001).

The AM algorithm draws samples (set of parameters) from the parameter space to generate probability distributions for the parameters. A sample in the parameter space has a value for each parameter and each parameter value is represented in the parameter space. The algorithm is used simultaneously for several independent chains that are parallel adaptations of the algorithmic process. The history of all chains is used for updating the proposal covariance matrix that describes how the parameters relate to one another. Our initial proposal covariance matrix had diagonal elements with 1/200 of each parameters range that was set as extensive. The first sample for each chain was chosen at random within this range. The algorithmic process can be described with few steps:

1. Draw a new sample (*x'*) of the parameter space from the vicinity of the current sample (*x*) using the current proposal covariance matrix.
2. Calculate the acceptance ratio (*a*) for the drawn sample. This is the value of a function (*f*), that is proportional to the desired probability distribution, at the drawn sample divided by the value at the current sample ($a = f(x')/f(x)$).
3. Accept the new candidate with the probability a. Update the covariance matrix and draw a new sample.

The cost function (1) used in this study for seasonal tuning is based on summary statistics of gross primary production (GPP) and evapotranspiration (ET) along with the maximum of leaf area index (LAI). Cost function (1) calculates the relative error in total GPP, ET and growing season maximum of LAI against observations and sums them up. Overlined variables refer to the mean value of that variable for a given period (calibration or validation).

$$cf = \left(1 - \frac{\overline{GPP}_{modelled}}{\overline{GPP}_{observed}}\right)^2 + \left(1 - \frac{\overline{ET}_{modelled}}{\overline{ET}_{observed}}\right)^2 + \left(1 - \frac{\max(LAI_{modelled})}{\max(LAI_{observed})}\right)^2 \quad (1)$$

The second cost function (2) is a slightly modified mean squared error estimate used for daily and half-hourly tuning. The pointwise differences in GPP and ET are divided by the mean values of the observed quantities, then squared, summed up and divided by the number of observations.

$$cf = \frac{1}{N_{GPP}} \sum \left(\frac{GPP_{modelled} - GPP_{observed}}{\overline{GPP}_{observed}} \right)^2 + \frac{1}{N_{ET}} \sum \left(\frac{ET_{modelled} - ET_{observed}}{\overline{ET}_{observed}} \right)^2 \tag{2}$$

As noted above JSBACH was used uncoupled from the other components of the full MPI-ESM. This has a tendency to lead to biased results in the model runs as has been recently studied by Dalmonech et al. (2015). Especially in the high latitudes evapotranspiration can be unrealistic during winter since night-time is longer and temperatures low. In order to improve the credibility of our results, we masked the evapotranspiration values of the coldest periods, and only took into account those from May to September for each year in both cost functions.

2.5 Parameter analysis

After tuning the model (explained in detail in the next section), we analysed different aspects of this process. Only class II and III parameters were part of this analysis since we wanted to exclude site specific parameters.

We calculated the correlation between different parameters to see how they affected one another and performed a principal component analysis (PCA) of the covariance matrices of the different tunings to reveal which parameters were the least identifiable. The PCA analysis transforms the covariance matrix into an orthogonal form where the eigenvector related to the greatest eigenvalue is the least convergent with the given data. This information could be extracted by analysing the parameters posterior probability distributions but PCA yields a simple, straightforward method for the same purpose.

We also wanted to examine which parameters contributed the most to the change in the cost function values as we switched from one parameter set to another. We call this method here “relative effectiveness” since we want to analyse the effect of the parameters to the cost function. For each tuned set of parameter values, the relative effectiveness of a parameter is calculated as follows:

1. Change one parameter from the set of tuned parameter values to a reference value and calculate the difference in the cost function for the changed set and the tuned set.

2. Return the changed parameter to the tuned value and repeat for all parameters. Sum up the differences.

3. The relative effectiveness for each parameter is the difference obtained from step 1 divided by the sum from step 2.

The relative effectiveness is similar to a class of methods commonly referred to as one-at-a-time (OAT) or one-factor-at-a-time (OFAT). These methods are generally used to acquire robust information about model behaviour when one parameter at a time is changed to a new or better value (see Murphy et al., 2004). Since we have already optimized the parameters as a group with the different cost functions, we use the method in reverse to see how the changes in the parameter values have affected the change in the cost function. This method does not reveal information about how well the parameters constrain the cost function

Nonlin. Processes Geophys. Discuss., doi:10.5194/npg-2016-21, 2016
Manuscript under review for journal Nonlin. Processes Geophys.
Published: 11 April 2016

Nonlinear Processes in Geophysics Discussions

(e.g. we could have a highly dominating parameter that would optimize to the default value and hence the relative effectiveness would be zero), rather which parameters contribute most to the change in cost function values.

3 Model tuning

The model was optimized for Hyytiälä with the AM algorithm using three different time scales: seasonal, daily and half-hourly tuning, which are described below.

3.1 Seasonal tuning

The fundamental motivation for the seasonal tuning is to ensure that the model reproduces the observed growing season maximum of LAI since we have previously noticed that JSBACH underestimates LAI on a site level (even the default value of Δ_{max} is lower than the measured maximum for Hyytiälä). The reason for this approach was to enhance the vegetation transpiration and to emphasize the model response to precipitation. We also want to ensure that the model performs adequately well in terms of seasonal cumulative GPP and ET. The seasonal tuning was done in three consecutive steps each using the cost function (1). The procedure is as follows:

1. Tuning of class I parameters with four independent chains each consisting of 3000 samples. This step required a 30-year spin up for each sample separately.
2. Testing of class II and III parameters each separately with 24 evenly separated values for an extensive range and tuning those parameters that didn't yield a negligible difference in the maximal and minimal values in the objective function. The consequent tuning was done with eight independent chains each consisting of 10 000 samples. A single spin up, common for all samples, used optimal parameter values from step 1 and default values for the rest of the parameters.
3. Retuning all the previously tuned parameters with eight independent chains each consisting of 10 000 samples. Initial covariance was generated from previous step and spin up was generated separately for each sample.

At the end of seasonal tuning, class I parameters were fixed and a single spin up was generated to be used with daily and half-hourly tuning. Vegetative fraction of a grid cell remained at its default value of 0.52 and carboxylation rate at 25 degrees Celsius was lowered to 45.0 (and electron transport rate to 85.5).

3.2 Daily and half-hourly tuning

The difference in daily and half-hourly tuning is the time interval used in the model output and observations in the cost function (2). For both tuning runs we first tested the response of class II and III parameters against the cost function (2) and removed those parameters that yielded only negligible or no response (as in step 2 in Seasonal tuning). The rest of the parameters were then tuned using eight independent chains each consisting of 10 000 samples.

Nonlin. Processes Geophys. Discuss., doi:10.5194/npg-2016-21, 2016
Manuscript under review for journal Nonlin. Processes Geophys.
Published: 11 April 2016

Nonlinear Processes in Geophysics
Open Access
Discussions

It should be noted that even though the cost function (2) formulation is the same for daily and half-hourly tuning, the values of the cost function are not directly comparable. Half-hourly tuning uses 48 approximately Gaussian distributed values (the diurnal cycle) in place of the one average daily value used by daily tuning. In practice the component and cost function values will be higher for half-hourly tuning.

3.3 Tuning for Sodankylä

After tuning the model for Hyytiälä we took the parameter set from seasonal tuning and retuned only the maximum LAI parameter (Δ_{max}) with the cost function (1) for Sodankylä. The other parameter values were taken from the respective Hyytiälä tuning runs and spin ups were generated similarly to Hyytiälä spin ups.

4 Results and discussion

The parameters and cost function components involved in the different phases of the optimization process need to be studied before the performance of the optimization method can be evaluated.

As noted above, we decided to reject the unreliable wintertime ET values. This masking leaves out the start of the growing season, which reduces the reliability of some of the tuned parameters, including all the LoGro phenology model parameters (class III), which mostly affect the timing of the spring event and regulate the development of the LAI towards the peak season. However, as a result of the tuning processes, all the analysed parameters were revealed to have unimodal posterior probability distributions, with different skewness's and deviations.

We analysed the correlations and effectiveness of the parameters in the seasonal, daily and half-hourly optimizations on the Hyytiälä site for the calibration period. We also analysed the contributions from the cost function components referring to ET, GPP and LAI and generated the time series and daily cycles of GPP and ET for both Hyytiälä and Sodankylä sites. For all these examinations, individual spin ups were generated using the optimized parameter values.

The parameter correlations (Table 2) do not reveal much information, which is common for larger systems where the underlying parameter dependencies are more complex. Usually more sophisticated methods are used to analyse the parameters, but we omit these examinations here since pairwise Kernel density estimates did not reveal any new insights.

The strongest correlation was between the ratio of leaf internal CO_2 concentration to external CO_2 (f_{C3}) and fraction of soil moisture above which transpiration is unaffected by soil moisture stress (w_{tsp}) in all the tunings. This positive correlation strengthens as we increase the temporal resolution (and the complexity of the underlying cost function). This is due to the carbon assimilation being limited by the amount of carbon available but also by a linear water stress factor (which takes the value of zero at the wilting point (w_{wilt}) and one at the w_{tsp}), which is checked at each time step. Most of the other parameters with high correlations are those of the LoGro phenology model, where we would expect high correlation since the parameters are intimately connected.

Approximately half of the parameters with high correlation are also the least identifiable (Table 3) with the given data and cost function. This means that the values these parameters acquire, as a result of the tuning process, are the most unreliable – it does not reflect on the parameters contribution to the cost function. The PCA merely highlights where most of the parametric unreliability lies.

The PCA analysis revealed that most of the unreliability is explained by a handful of parameters. Disregarding those of the LoGro phenology model, the two most dominantly unreliable parameters in every tuning were the fraction depicting relative humidity based on soil dryness (w_{hum}) and the maximum field capacity of the skin reservoir (w_{skin}). Both of these parameters affect the amount of water available for evaporation from bare soil and are both subject to changes in other parameters. Bare soil evaporation is also dominated by vegetative transpiration, which explains why these two parameters are the most unreliable.

4.1 The parameters and their relative effectiveness

The default and optimized parameter values from the different tuning metrics are presented in Table 4 along with their relative effectiveness. The reference values for seasonal tuning are the default values. Since we fixed class I parameters with seasonal tuning, the realistic reference values for daily and half-hourly tunings are the seasonal parameter values. Here we note that using one spin up for all daily and half-hourly optimization runs is computationally justifiable but generates errors as the general spin up differs from those generated by the optimized parameters. These errors give rise to e.g. the negative relative effectiveness values in daily and half-hourly parametrizations.

Most seasonally tuned parameters are near their default values and the most effective parameters are the fraction of soil moisture above which transpiration is unaffected by soil moisture stress (w_{tsp}), the fraction of soil moisture at permanent wilting point (w_{pwp}) and the fraction of field capacity above which fast drainage occurs (w_{dr}). For daily and half-hourly tunings the most important parameters are the ratio of leaf internal CO_2 concentration to external CO_2 (f_{C3}) and the fraction depicting relative humidity (w_{hum}). It should be noted that w_{hum} was one of the least identifiable parameters for seasonal tuning. Given into account the importance of these parameters on transpiration and soil moisture estimations, we took a closer look at modelled soil moisture and evapotranspiration components for the calibration period (taking into account only values from May to September for each year as explained in chapter Uncoupled model runs).

When we compare the model output streams with seasonal against those with default parametrization, we notice that the average evapotranspiration for the calibration period has increased 15%. Most of this is due to added transpiration (18% increase) but also increased evaporation (6%). In addition drainage was accelerated by 11%. These increases are mostly compensated by a 15% reduction in average soil moisture. In addition soil moisture values that are under the limit when transpiration is affected by soil moisture stress (below the value of w_{tsp}) increased 2.3%.

The daily and half-hourly tunings lower the average evapotranspiration by 22% and 35% respectively when compared to the seasonal values. Transpiration is decreased by 28% and 37% whereas evaporation is increased by 0.5% and decreased by 28%, respectively for daily tuning and half-hourly tuning. Soil moisture is increased by 11% and 8% and the amount of values below w_{tsp} is decreased by 62% for daily tuning and increased by 7% for half-hourly tuning. As a curiosity, both the adjustment parameter in stability functions (c_b) and the fraction of precipitation intercepted by canopy (p_{int}) have been significantly increased with daily tuning and returned to seasonally tuned values with half-hourly tuning.

4.2 The cost function components

Using the optimized values (parametrizations) we calculated the components of each cost function for Hyytiälä calibration period and Hyytiälä and Sodankylä validation period (Table 5).

Firstly we note that with the default parameters L_1 dominates Σ_1 for Hyytiälä and contributes to approximately 90% to its value. As expected the L_1 for Sodankylä is not as dominant as for Hyytiälä since the measured maximum of LAI is roughly half as large, which directly lowers the LAI component in cost function (1). The L_1 contribution is significantly reduced with the seasonally tuned parameters as was our intention and even though LAI plays no part in daily and half-hourly tunings, the differences in the maximum value are negligible.

Secondly the value of E_1 component (error in seasonal ET) with default parametrization is significantly increased in daily and especially half-hourly parametrizations. Simultaneously the value of G_1 is significantly lowered. The component values for seasonal parametrization are better than the default values with the exception of E_1 for Hyytiälä validation period.

Thirdly for cost function (2) the pairwise ratio of dominating E_i or G_i components in all tunings is 5:1. On average E_2/E_3 contributes to approximately 60% of Σ_2/Σ_3. This translates to ET being twice as significant as GPP in cost function (2). The main reason for ET dominating GPP is that ET is a more turbulent flux than GPP. The daily and half-hourly tunings themselves work as intended as they lower the corresponding cost function value. It is noteworthy to mention that the G_2 component gets its lowest value for both validation periods with the half-hourly parametrization even though G_2 calculates GPP errors on a daily scale.

Lastly we examine how the algorithm and cost functions have performed. The best parameter set (lowest cost function value) for a given cost function, in each of the three different periods (HC, HV, SV), is the same that was used in the corresponding tuning process. For example the lowest value for Σ_1 (cost function for seasonal tuning) in Sodankylä validation period (0.07) coincides with the seasonally tuned parameters. This holds true for every cost function with the exception of Σ_1 for Hyytiälä validation period, where the lowest value is reached with the daily tuned parameters (we note that the absolute difference between daily and seasonally tuned parameters is small). Hence we can confidently state that the algorithm and cost functions have performed as intended, especially since the optimised parameters work for Sodankylä as well, where no optimization (besides the site specific maximum of LAI) was applied.

4.3 Time series

The overall structure of the model time series was not affected by the parametrizations obtained with different tunings (Fig. 1 and Fig. 2). Some time series characteristics have been enhanced and others reduced but the timing of the peaks and dips in GPP and ET are the same as before.

The best seasonal performance was obtained by seasonal tuning as we previously noticed from the cost function components (Table 5). Even though the optimization is done on the seasonal level, especially the GPP cycle is noticeably improved from that generated by the default parameters. This tuning also gives rise to the most stable (least fluctuating) water use efficiency

Nonlin. Processes Geophys. Discuss., doi:10.5194/npg-2016-21, 2016
Manuscript under review for journal Nonlin. Processes Geophys.
Published: 11 April 2016

Nonlinear Processes in Geophysics
Discussions
Open Access

(WUE), when calculated as a pointwise ratio of GPP and ET. We use WUE here only as a diagnostic variable to examine the balance between the GPP and ET.

When compared to the seasonal tuning, the daily tuning is worse on the seasonal scale and lowers both the ET and GPP cycles. WUE follows the observations better but starts to give rise to some fluctuation. With half-hourly tuning this behaviour is further enhanced and especially ET is lowered to too low levels which manifests the high WUE values. The worsening in the model time series with daily and half-hourly tunings are explained by biases in the diurnal cycle.

4.4 Diurnal cycles

Average diurnal cycles with different parametrizations (Fig. 3) show that modelled night-time ET values are too low when compared to the observed and this behaviour was not affected by the tunings. Low night-time values are compensated by too high midday values in the default and seasonal tuning so that the average daily and seasonal values are on an acceptable level. For the daily and half-hourly tuning, the algorithm lowers the daytime values, which results in too low average daily and half-hourly values. It is noteworthy to mention that with the default setting we get too low GPP for Hyytiälä but too high for Sodankylä. The unrealistic wintertime and the biased night-time ET values actually have the same origin. Since we do not have the coupling from the land surface model (LSM) back to the atmosphere, we get an erroneous energy balance as we lose the energy released by condensation.

Disregarding the default parametrization we notice that seasonal parametrization show the highest values, daily in the middle and half-hourly show the lowest values. Daily parametrization reproduces the observations for average diurnal cycle better than the others in every occasion except the GPP for Sodankylä, where half-hourly tuning is better (verified by pointwise RMSE from the average diurnal cycle). We also notice that Sodankylä daily patterns, and to some extent Hyytiälä as well, are slightly out of phase. Our current understanding is that this is (at least partly) due to a slightly misaligned sensor (which can cause significant errors on high latitudes), measuring radiation fluxes. Fortunately this affects mainly the cost function for half-hourly tuning since it is the only one operating on the densest half-hourly timescale.

4.5 Dry event

Dry period in the summer 2006 can be clearly located by the massive drawdown in observed GPP, and to a lesser extent in ET, at Hyytiälä (Fig. 1). In a closer look at this event (Fig. 4) it is evident that none of our parametrization schemes were able to capture it correctly. As it was with the time series, the overall structure of the daily time series during this event remains the same (there are no divergent aspects in the model output between the different tunings).

During the drought event (defined here as 31.7.–15.8.2006) the soil moisture is on average 27% lower for default, daily and half-hourly tuning and 40% lower for seasonal tuning when compared to the corresponding values from other years – seasonal tuning has the lowest overall soil moisture. During this event the modelled soil moisture decreases monotonically for all tunings and reaches the lowest values on 13th of August, after which it starts to rise. During the period the modelled ET and GPP are predominantly higher than the observations. WUE on the other hand follows the “observations” remarkably well and deviates from the observed only towards the end of the event when modelled ET drops to near zero values, coinciding with the lowest modelled soil moisture values.

5 Conclusions

Initially we tuned the model to produce near measured seasonal ET, GPP and especially maximum LAI to enhance the vegetation transpiration and to emphasize the response to precipitation. This was done successfully with seasonal tuning in the hopes of bringing forth the underlying model responses to dryness. With the consecutive daily and half-hourly tunings, we managed to improve the average diurnal cycles of both ET and GPP, but failed in reproducing the low ET and GPP levels during the dry event in 2006. Effectively we first (seasonal tuning) transferred water from soil moisture into (too high levels of) ET, and later (with daily and half-hourly tunings) transferred some of it back.

In addition to the site specific parameters, the most effective parameters in the seasonal tuning were the fraction of soil moisture above which transpiration is not affected by soil moisture stress (w_{tsp}) and the critical fraction of field capacity above which fast drainage occurs for soil water content (w_{dr}). The reduction in ET and GPP was mostly accounted for by lowering the approximate ratio of leaf internal CO_2 concentration to external CO_2 (f_{C3}), which reduces the amount of carbon available for photosynthesis. For daily tuning ET was further reduced by the increase of the fraction of precipitation intercepted by canopy (p_{int}) and lower relative humidity fraction (w_{hum} – air humidity is based on soil dryness).

Despite the fact that we were unable to enhance the dry response of the model, we are confident in saying that the algorithm itself worked well and performed as intended with the daily tuning providing the most reduction in model-data mismatch. Recently Knauer et al. (2015) found canopy conductance formulation to be a key factor in prescribing the transfer of carbon and water between terrestrial biosphere and the lower atmosphere. Further studies into enhancing the dry response in JSBACH are needed and these studies should include revisiting canopy and stomatal conductance formulations.

Author contributions. T. Aalto, T. Markkanen and S. Hagemann chose the parameters in the optimization process. M. Aurela and I. Mammarella provided knowledge on the observations. J. Susiluoto provided the algorithm testbed and J. Mäkelä integrated the model into the testbed, run the experiments and prepared the manuscript with contributions from all co-authors.

Acknowledgements. This work was funded by the European Commission's 7th Framework Programme, under Grant Agreement number 282672, EMBRACE project, and the Nordic Centre of Excellence 'Tools for Investigating Climate Change at High Northern Latitudes' (eSTICC) under the Nordic Top-Level Research Initiative. This work was also supported by the Academy of Finland Center of Excellence (no. 272041), ICOS-Finland (no. 281255), and ICOS-ERIC (no. 281250) funded by Academy of Finland. This work used eddy covariance data acquired and shared by the FLUXNET community, including these networks: AmeriFlux, AfriFlux, AsiaFlux, CarboAfrica, CarboEuropeIP, CarboItaly, CarboMont, ChinaFlux, Fluxnet-Canada, GreenGrass, ICOS, KoFlux, LBA, NECC, OzFlux-TERN, TCOS-Siberia, and USCCC. The FLUXNET eddy covariance data processing and harmonization was carried out by the ICOS Ecosystem Thematic Center, AmeriFlux Management Project and Fluxdata project of FLUXNET, with the support of CDIAC, and the OzFlux, ChinaFlux and AsiaFlux offices.

References

Aalto T., Ciais P., Chevillard A. and Moulin C.: Optimal determination of the parameters controlling biospheric CO_2 fluxes over Europe using eddy covariance fluxes and satellite NDVI measurements, Tellus, 56B, 93–104, doi:10.3402/tellusb.v56i2.16413, 2004.

Aurela M.: Carbon dioxide exchange in subarctic ecosystems measured by a micrometeorological technique, Finnish Meteorological Institute Contributions, 51, 2005.

Aurela M., Lohila A., Tuovinen J.P., Hatakka J., Riutta T. and Laurila T.: Carbon dioxide exchange on a northern boreal fen, Boreal Environ. Res., 14: 699–710. 2009.

Baldocchi D.D.: Assessing the eddy covariance technique for evaluating carbon dioxide exchange rates of ecosystems: past, present and future, Glob. Change Biol., 9, 479–492, doi:10.1046/j.1365-2486.2003.00629.x, 2003.

Boé J. and Terray L.: Uncertainties in summer evapotranspiration changes over Europe and implications for regional climate change, Geophys. Res. Lett., 35, L05702, doi:10.1029/2007GL032417, 2008.

Dalmonech D., Zaehle S., Schürmann G. J., Brovkin V., Reick C. and Schnur R.: Separation of the Effects of Land and Climate Model Errors on Simulated Contemporary Land Carbon Cycle Trends in the MPI Earth System Model version 1, J. Climate, 28, 272–291, doi:10.1175/JCLI-D-13-00593.1, 2015.

Farquhar G.D., Caemmerer von S. and Berry J.A.: A Biochemical Model of Photosynthetic CO_2 Assimilation in Leaves of C3 species, Planta, 149, 78–90, doi:10.1007/BF00386231, 1980.

Haario H., Saksman E. and Tamminen J.: An adaptive Metropolis algorithm, Bernoulli, 7, 223–242, 2001.

Hagemann S.: An improved land surface parameter dataset for global and regional climate models, Max Planck Institute for Meteorology Report, 336, 2002.

Hagemann S. and Stacke T.: Impact of the soil hydrology scheme on simulated soil moisture memory, Clim. Dynam., 44, 1731–1750, doi:10.1007/s00382-014-2221-6, 2015.

Kaminski T., Knorr W., Schürmann G., Scholze M., Rayner P.J., Zaehle S., Blessing S., Dorigo W., Gayler V., Giering R., Gobron N., Grant J.P., Heimann M., Hooker-Stroud A., Houweling S., Kato T., Kattge J., Kelley D., Kemp S., Koffi E. N., Köstler C., Mathieu P.-P., Pinty B., Reick C. H., Rödenbeck C., Schnur R., Scipal K., Sebald C., Stacke T., Terwisscha van Scheltinga A., Vossbeck M., Widmann H. and Ziehn T.: The BETHY/JSBACH Carbon Cycle Data Assimilation System: experiences and challenges, J. Geophys. Res-Biogeo., 118, 1414–1426, doi:10.1002/jgrg.20118, 2013.

Kattge J., Knorr W., Raddatz T. and Wirth C.: Quantifying photosynthetic capacity and its relationship to leaf nitrogen content for global-scale terrestrial biosphere models. Glob. Change Biol., 15, 976–991, doi:10.1111/j.1365-2486.2008.01744.x, 2009.

Knauer J., Werner C. and Zaehle A.: Evaluating stomatal models and their atmospheric drought response in a land surface scheme: A multibiome analysis, J. Geophys. Res-Biogeo., 120, 1894–1911, doi:10.1002/2015JG003114, 2015.

Knorr W.: Satellite Remote Sensing and Modelling of the Global CO_2 Exchange of Land Vegetation: A Synthesis Study, Max-Planck-Institut für Meteorologie Examensarbeit, 49, 1997.

Knorr W. and Kattge E.: Inversion of terrestrial ecosystem model parameter values against eddy covariance measurements by Monte Carlo sampling, Glob. Change Biol., 11, 1333–1351, doi:10.1111/j.1365-2486.2005.00977.x, 2005.

Kolari P., Pumpanen J., Rannik Ü., Ilvesniemi H., Hari P. and Berninger F.: Carbon balance of different aged Scots pine forests in Southern Finland, Glob. Change Biol., 10, 1106–1119, doi:10.1111/j.1529-8817.2003.00797.x, 2004.

Kolari P., Kulmala L., Pumpanen J., Launiainen S., Ilvesniemi H., Hari P. and Nikinmaa E.: CO_2 exchange and component CO_2 fluxes of a boreal Scots pine forest, Boreal Environ. Res., 14, 761–783, 2009.

Mammarella I., Launiainen S., Gronholm T., Keronen P., Pumpanen J., Rannik Ü. and Vesala T.: Relative Humidity Effect on the High-Frequency Attenuation of Water Vapor Flux Measured by a Closed-Path Eddy Covariance System, J. Atmos. Ocean. Tech., 26, 1856–1866, doi:10.1175/2009JTECHA1179.1, 2009.

Matheny A.M., Bohrer G., Stoy P.C., Baker I.T., Black A.T., Desai A.K., Dietze M.C., Gough C.M., Ivanov V.Y., Jassal R.S., Novick K.A., Schäfer K.V.R. and Verbeeck H.: Characterizing the diurnal patterns of errors in the prediction of evapotranspiration by several land-surface models: An NACP analysis, J. Geophys. Res-Biogeo., 119, 1458–1473, doi:10.1002/2014JG002623, 2014.

Mueller B. and Seneviratne S.I.: Systematic land climate and evapotranspiration biases in CMIP5 simulations, Geophys. Res. Lett., 41, 128–134, doi:10.1002/2013GL058055, 2014.

Murphy J.M., Sexton D.M.H, Barnett D.N., Jones G.S., Webb M.J, Collins M. and Stainforth D.A.: Quantification of modelling uncertainties in a large ensemble of climate change simulations, Nature, 430, 768–772, doi:10.1038/nature02771, 2004.

Peltoniemi M., Pulkkinen M., Aurela M., Pumpanen J., Kolari P. and Mäkelä A.: A semi-empirical model of boreal-forest gross primary production, evapotranspiration, and soil water – calibration and sensitivity analysis, Boreal Environ. Res., 20, 151–171, 2015a.

Peltoniemi M., Markkanen T., Härkönen S., Muukkonen P., Thum T., Aalto T. and Mäkelä A.: Consistent estimates of gross primary production of Finnish forests – comparison of estimates of two process models, Boreal Environ. Res., 20, 196–212, 2015b.

Reick C.H., Raddatz T., Brovkin V. and Gayler V.: Representation of natural and anthropogenic land cover change in MPI-ESM, Journal of Advances in Modeling Earth Systems, 5, 1–24, doi:10.1002/jame.20022, 2013.

Santaren D., Peylin P., Bacour C., Ciais P. and Longdoz B.: Ecosystem model optimization using in situ flux observations: benefit of Monte Carlo versus variational schemes and analyses of the year-to-year model performances, Biogeosciences, 11, 7137–7158, doi:10.5194/bg-11-7137-2014, 2014.

Scharnagl B., Vrugt J.A., Vereecken H. and Herbst M.: Inverse modelling of in situ soil water dynamics: investigating the effect of different prior distributions of the soil hydraulic parameters, Hydrol. Earth Syst. Sc., 15, 3043–3059, doi:10.5194/hess-15-3043-2011, 2011.

Schulze E.D., Kelliher F.M., Korner C., Lloyd J. and Leuning R.: Relationships among Maximum Stomatal Conductance, Ecosystem Surface Conductance, Carbon Assimilation Rate, and Plant Nitrogen Nutrition: A Global Ecology Scaling Exercise, Annu. Rev. Ecol. Syst., 25, 629–662, 1994.

Sellers P.J. Canopy reflectance, photosynthesis and transpiration, Int. J. Remote Sens., 6, 1335–1372, 1985.

Suni T., Rinne J., Reissell A., Altimir N., Keronen P., Rannik Ü., Dal Maso M., Kulmala M. and Vesala T.: Longterm measurements of surface fluxes above a Scots pine forest in Hyytiälä, southern Finland, 1996–2001, Boreal Environ. Res., 8, 287–301, 2003.

Thum T., Aalto T., Laurila T., Aurela M., Kolari P. and Hari P.: Parametrization of two photosynthesis models at the canopy scale in northern boreal Scots pine forest, Tellus, 59B, 874–890, doi:10.1111/j.1600-0889.2007.00305.x, 2007.

Thum T., Aalto T., Laurila T., Aurela M., Lindroth A. and Vesala T.: Assessing seasonality of biochemical CO_2 exchange model parameters from micrometeorological flux observations at boreal coniferous forest, Biogeosciences, 5, 1625–1639, 2008.

Vesala T., Suni T., Rannik Ü., Keronen P., Markkanen T., Sevanto S., Grönholm T. Smolander S., Kulmala M. Ilvesniemi H., Ojansuu R., Uotila A., Levula J., Mäkelä A., Pumpanen J., Kolari P., Kulmala L., Altimir N., Berninger F., Nikinmaa E. and Hari P.: Effect of thinning on surface fluxes in a boreal forest, Global Biogeochem. Cy., 19, GB2001, doi:10.1029/2004GB002316, 2005.

Wu S., Jansson P. and Kolari P.: Modeling seasonal course of carbon fluxes and evapotranspiration in response to low temperature and moisture in a boreal Scots pine ecosystem, Ecol. model., 222, 3103–3119, doi:10.1016/j.ecolmodel.2011.05.023, 2011.

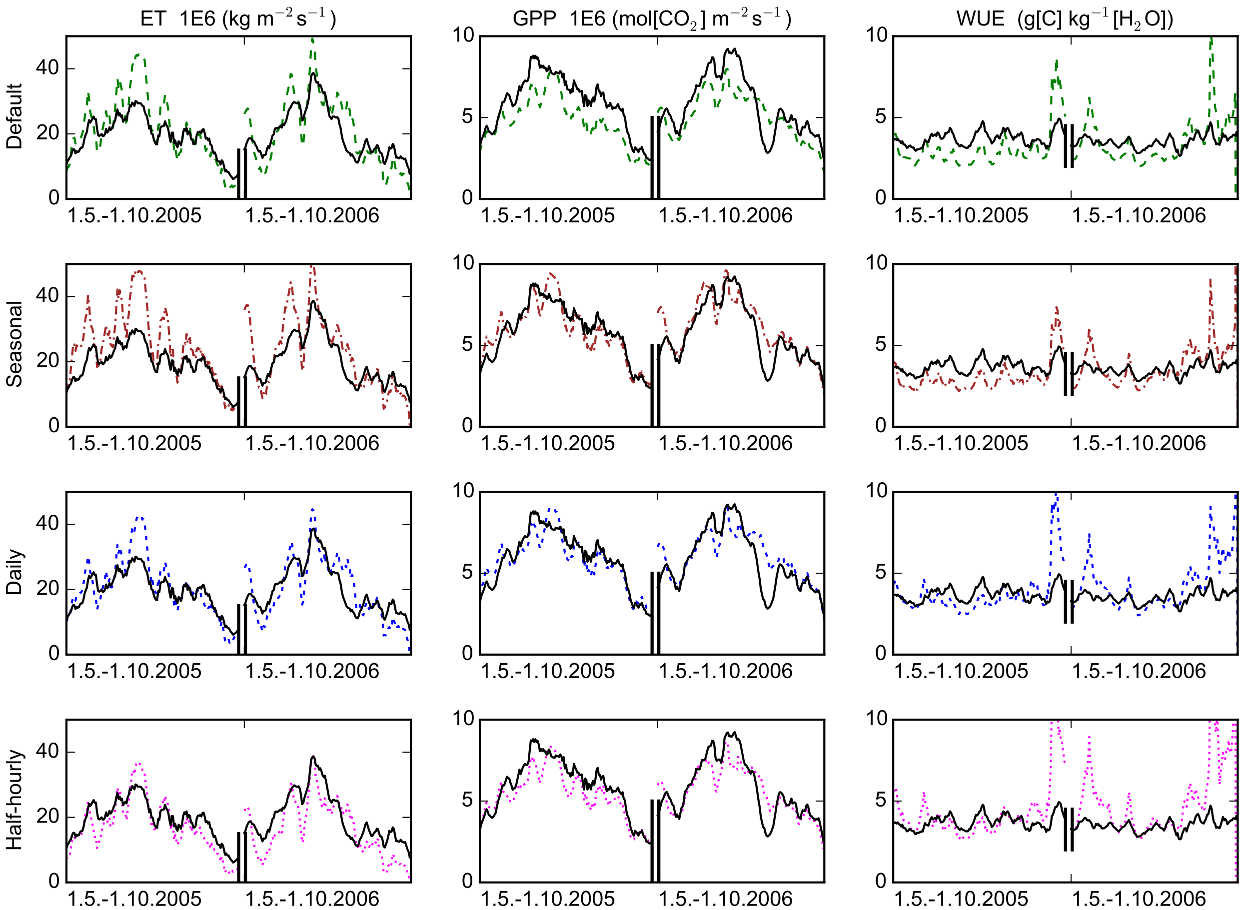

Figure 1. Hyytiälä 7-day running mean time series for different tunings for the first two summers of the validation period. Solid black line represents the observations.

Nonlin. Processes Geophys. Discuss., doi:10.5194/npg-2016-21, 2016
Manuscript under review for journal Nonlin. Processes Geophys.
Published: 11 April 2016

Nonlinear Processes in Geophysics
Discussions
Open Access

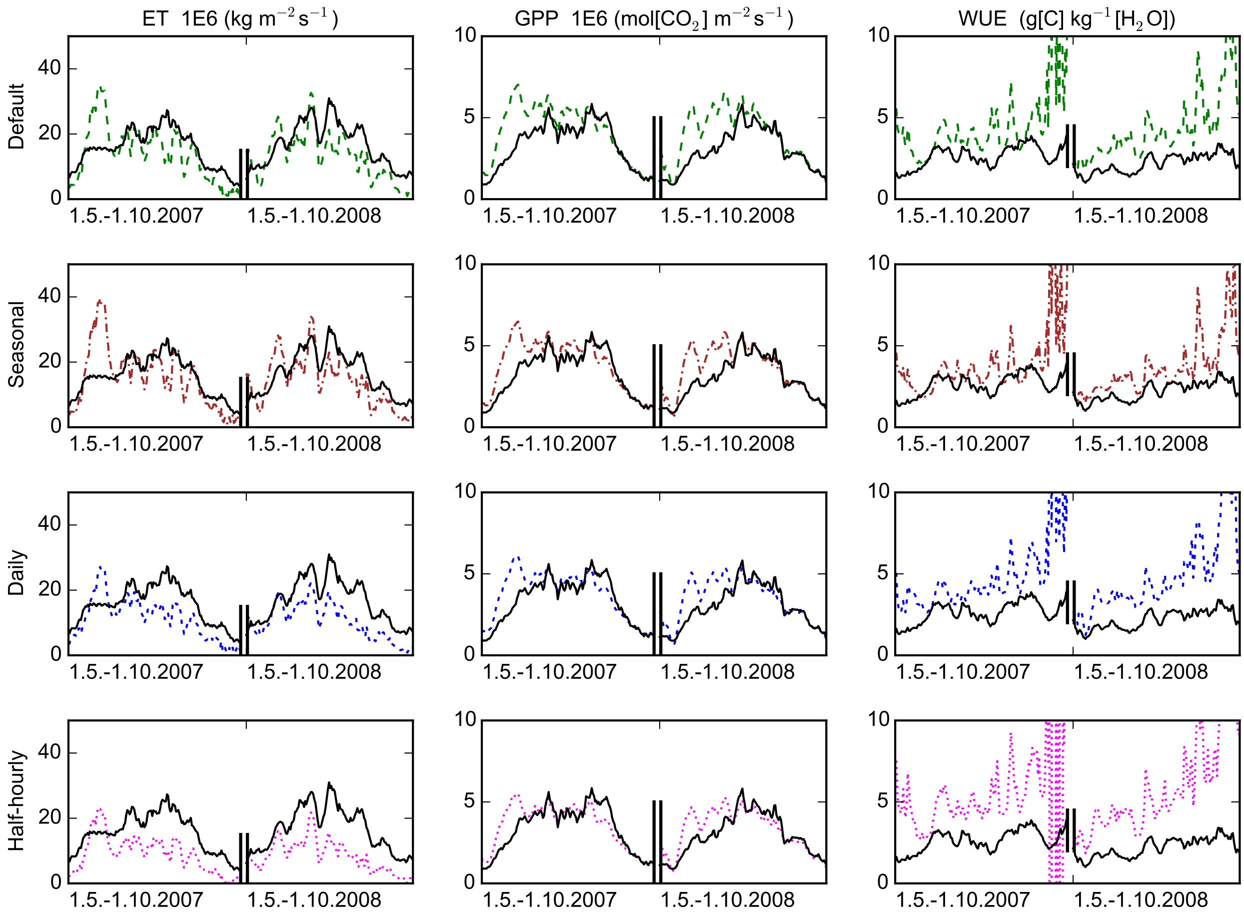

Figure 2. Sodankylä 7-day running mean time series for different tunings for the last two summers of the validation period. Solid black line represents the observations.

Nonlin. Processes Geophys. Discuss., doi:10.5194/npg-2016-21, 2016
Manuscript under review for journal Nonlin. Processes Geophys.
Published: 11 April 2016

Nonlinear Processes in Geophysics
Discussions
Open Access

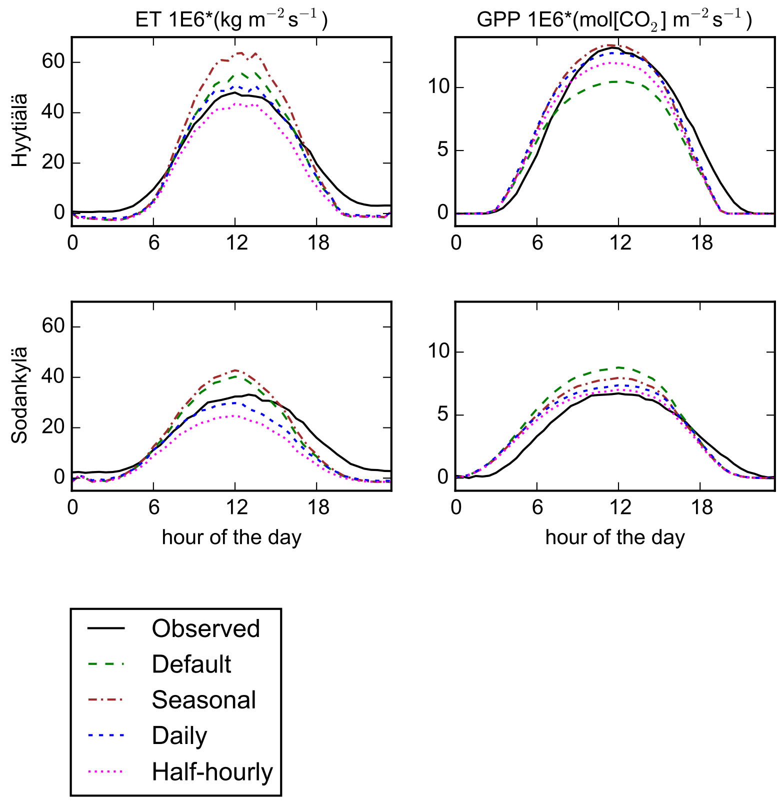

Figure 3. Average diurnal cycle from May to September for the validation period.

Nonlin. Processes Geophys. Discuss., doi:10.5194/npg-2016-21, 2016
Manuscript under review for journal Nonlin. Processes Geophys.
Published: 11 April 2016

Nonlinear Processes in Geophysics
Discussions
Open Access

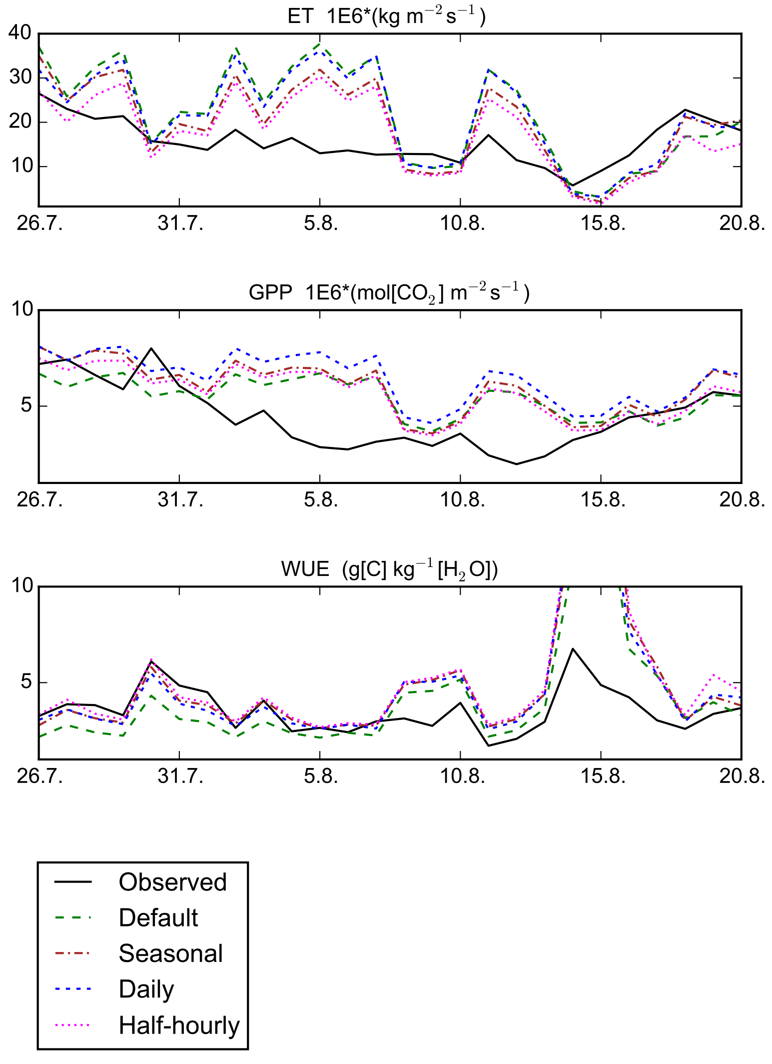

Figure 4. Daily averages for ET, GPP and WUE on a dry event in 2006 for Hyytiälä.

Nonlin. Processes Geophys. Discuss., doi:10.5194/npg-2016-21, 2016
Manuscript under review for journal Nonlin. Processes Geophys.
Published: 11 April 2016

Nonlinear Processes in Geophysics
Open Access
Discussions

Table 1. Parameter descriptions. *These parameters were tested but yielded no or only minimal response to cost functions and were thus removed from the trial.

Parameter	Class	Desciption
Δ_{max}	I	Maximum all-sided leaf area index that vegetation can reach.
J_{max}	I	Farquhar model maximum carboxylation rate at 25°C of the enzyme Rubisco (coupled with maximum electron transport rate at 25°C with a factor of 1.9).
veg_{max}	I	Fraction of vegetative soil in a grid cell. The rest is bare soil.
α_q	II	Farquhar model efficiency for photon capture at 25°C.
c_b	II	Adjustment parameter used in stability functions for momentum and heat.
f_{C3}	II	Ratio of C3-plant internal/external CO_2 concentration.
p_{int}	II	Fraction of precipitation intercepted by the canopy.
w_{dr}	II	Critical fraction of field capacity above which fast drainage occurs for soil water content.
w_{hum}	II	Fraction depicting relative humidity based on soil dryness.
w_{pwp}	II	Fraction of soil moisture at permanent wilting point.
w_{skin}	II	Maximum water content of the skin reservoir of bare soil.
w_{tsp}	II	Fraction of soil moisture above which transpiration is not affected by soil moisture stress.
s_{sm}*	II	Depth for correction of surface temperature for snow melt.
T_{alt}	III	LoGro phenology: alternating temperature. Cutoff temperature used for calculating heatsum to determine the spring event (when greater or equal to critical heatsum) and the number of chill days since the last autumn event.
C_{decay}*	III	LoGro phenology: memory loss parameter for chill days.
S_{min}	III	LoGro phenology: minimum value of critical heat sum.
S_{range}*	III	LoGro phenology: maximal range of critical heat sum.
T_{ps}	III	LoGro phenology: pseudo soil temperature as an average air temperature with exponential memory loss.

Table 2. Highest correlations between parameters.

Tuning	parameters		r
seasonal	f_{C3}	w_{tsp}	0.49
	T_{alt}	α_q	0.40
daily	f_{C3}	w_{tsp}	0.52
	w_{dr}	w_{tsp}	0.52
	T_{alt}	T_{ps}	-0.48
	T_{alt}	S_{min}	0.47
half-hourly	f_{C3}	w_{tsp}	0.68
	p_{int}	w_{skin}	-0.44

Nonlin. Processes Geophys. Discuss., doi:10.5194/npg-2016-21, 2016
Manuscript under review for journal Nonlin. Processes Geophys.
Published: 11 April 2016

Table 3. Significant components of principal component analysis for the different tunings. Weight is the eigenvalue for that component squared and divided by the sum of the squares of all eigenvalues. The given parameters are the most dominant within the component and ratio is how many times larger the factor related to the first parameter is when compared to that of the second. Coverage reveals how much of the component is accounted for by the given parameters.

Component	weight	parameters		ratio	coverage
seasonal 1.	0.996	w_{hum}	w_{skin}	2.1	$> 99\%$
daily 1.	0.717	T_{ps}	w_{skin}	1.4	$> 99\%$
daily 2.	0.261	w_{hum}	w_{tsp}	2.3	$> 99\%$
half-hourly 1.	0.530	T_{ps}	-	-	$> 99\%$
half-hourly 2.	0.310	w_{skin}	w_{hum}	1.7	96%
half-hourly 3.	0.121	T_{alt}	-	-	$> 99\%$

Table 4. Default and optimized parameter values (if no value is given, the parameter was not part of that tuning and the default value was used instead). The percentage next to a parameter value is the effectiveness of that parameter for that tuning. The reference values for seasonal tuning are the default values and for daily and half-hourly tunings the seasonal values.

Parameter	default	seasonal		daily		half-hourly	
α_q	0.28	0.26	7%	0.30	3%	0.27	1%
c_b	5.0	-	-	8.8	7%	5.0	0%
f_{C3}	0.87	0.88	8%	0.72	70%	0.76	68%
p_{int}	0.25	0.27	1%	0.49	4%	0.27	0%
w_{dr}	0.9	0.79	14%	0.87	1%	0.75	-1%
w_{hum}	0.5	0.54	1%	0.25	14%	0.37	22%
w_{pwp}	0.35	0.28	10%	0.34	0%	0.31	-1%
w_{skin}	2.0E-4	3.1E-4	6%	3.0E-4	0%	2.2E-4	6%
w_{tsp}	0.75	0.64	53%	0.60	1%	0.75	3%
T_{alt}	4.0	8.1	0%	6.9	1%	6.9	2%
S_{min}	10.0	-	-	23.0	-0%	14.7	-0%
T_{ps}	10.0	-	-	21.0	-0%	12.4	-0%

Nonlin. Processes Geophys. Discuss., doi:10.5194/npg-2016-21, 2016
Manuscript under review for journal Nonlin. Processes Geophys.
Published: 11 April 2016

Nonlinear Processes in Geophysics
Discussions
Open Access

Table 5. Cost function components for each parametrization for Hyytiälä calibration (HC), validation (HV) and Sodankylä validation (SV) periods. The highlighted values are part of the cost function used for that parametrization. L_1, E_1 and G_1 are the LAI, ET and GPP components in cost function (1), represented by Σ_1. Likewise E_2 and G_2 are the components in cost function (2) for daily values (Σ_2), whereas E_3 and G_3 are for half-hourly values (Σ_3). Note that the values of Σ_2 and Σ_3 are not directly comparable.

		L_1	E_1	G_1	E_2	G_2	E_3	G_3	Σ_1	Σ_2	Σ_3
HC	default	0.396	0.021	0.036	0.306	0.191	1.126	0.681	0.45	0.50	1.8
	seasonal	5.0E-5	1.7E-4	5.7E-6	0.343	0.161	1.326	0.720	2.3E-4	0.50	2.0
	daily	7.4E-5	0.055	1.4E-4	0.206	0.149	0.906	0.683	0.06	0.36	1.6
	half-hourly	1.0E-4	0.128	5.4E-3	0.276	0.151	0.864	0.661	0.13	0.43	1.5
HV	default	0.396	0.002	0.028	0.226	0.157	1.027	0.479	0.43	0.38	1.5
	seasonal	9.3E-5	0.011	7.5E-4	0.300	0.134	1.370	0.459	0.01	0.43	1.8
	daily	1.4E-4	0.007	3.5E-4	0.164	0.124	0.981	0.446	7E-3	0.29	1.4
	half-hourly	1.1E-4	0.058	2.9E-3	0.182	0.118	0.748	0.412	0.06	0.30	1.2
SV	default	0.108	4.0E-3	0.140	0.423	0.596	1.660	1.795	0.25	1.02	3.5
	seasonal	5.9E-3	1.8E-5	0.068	0.467	0.411	1.786	1.429	0.07	0.88	3.2
	daily	6.1E-3	0.063	0.048	0.289	0.352	1.258	1.294	0.12	0.64	2.6
	half-hourly	5.9E-3	0.164	0.022	0.379	0.290	1.246	1.185	0.19	0.67	2.4